

x. Insertion Quadrupoles

Three large-aperture (13 cm) quadrupoles are located on either side of all six of the RHIC crossing points. The three quadrupoles are close together as a "triplet" and perform the final strong focusing for the experiments. Because the transverse beam sizes are at their ring-wide maximum in the experimental triplets when β^* is small, the ultimate luminosity performance of RHIC depends both on the optimum arrangement of these quadrupoles, and also on achieving the highest possible magnetic field quality.

In the present lattice, a total number of 72 large-aperture quadrupole magnets are needed in six insertions. The maximum operating gradient required is ~ 48 T/m and the magnetic length is 1.44 m in 24 Q1, 3.40 m in 24 Q2, and 2.10 m in 24 Q3 quadrupoles. The outer dimensions of these quadrupoles are determined by the beam spacing at the entrance of the first two quadrupoles on either side of the crossing point. The minimum radial separation between the inner and outer beams at Q1 is 424 mm.

Basic Design Parameters

Table 10-1 summarizes the basic design parameters of the large-aperture quadrupoles. Following are some basic design features which were developed after optimizing the magnetic and mechanical design of this quadrupole:

A circular iron yoke with an outer diameter of 350.5 mm (363.2 mm including the shell) is used in these quadrupoles. This leaves a minimum separation of ~ 61 mm between the inner and outer Q1 quadrupoles.

Coil pre-compression is obtained by pressing and keying the yoke halves.

The single layer coil uses the 36-strand cable developed for the outer layer of the SSC 50 mm aperture dipole magnet. The parameters of this cable are given in Tables 2-3 and 2-4.

An RX630 spacer is used between the coil and the yoke, just as it is used in the arc dipole magnets. The azimuthal position of the coil is defined by a notch at the midplane of the magnet.

The iron aperture is a modified circle in order to reduce iron saturation effects. The radius increases from 87 mm at 0° to 92 mm at 30° in the first quadrant, to return to 87 mm at 60° . These cutouts are symmetric in the other quadrants, as shown in Fig. 10-1, which shows a cross section of

the coil and yoke. This iron geometry holds the change in $b_{s'}$ and $b_{y'}$ over the nominal operating range to about 0.3 units.

The outer radius of the plastic spacer also changes from 87 to 92 mm. However, Fig. 10-1 shows that a space is left between the plastic spacer and the iron at the eight locations where the circle radius changes. These spaces were used to install tuning shims for field quality correction after the magnets are built.

Two of the four large non-circular holes in the yoke are used for helium flow. The other two are primarily used for the dipole bus. The holes are located to preserve quadrupole symmetry, and thus minimize saturation effects. The net hydraulic impedance is about the same as that of the four circular holes in the arc magnets.

The beam tube is a seamless stainless steel 316LN tube with a bare outer diameter of 121 mm and is wrapped with 25 μm Kapton with 60% overlay.

The iron yoke was designed to maintain quadrupole symmetry so far as possible, while also allowing for the necessary bus work, helium circulation, mechanical features, and saturation control. The yokes are enclosed in a stainless steel shell, along with corrector magnets, to give mechanical rigidity and helium containment. The technique of applying weld stripes to the shell to reduce twist, first used on the arc dipoles, was applied here as well. The rms twist on the Q2's was reduced from 1-2 mrad to less than 0.5 mrad [CO97a]. These cold masses as well as those in the neighboring ring and the adjoining D0 bending magnets were all built into a common vacuum tank in-situ.

Table 10-1. Design Parameters of RHIC 13 cm Bore Quadrupoles

Parameter	Value
Coil aperture	130 mm
Number of turns per pole	27
Number of magnets in machine	72
Magnetic length, Q1, Q2, Q3	1.44, 3.40, 2.10 m
Iron inner diameter at midplane	174 mm
Iron inner diameter at pole	184 mm
Iron outer diameter	350.5 mm
Spacer thickness at midplane	10 mm
Spacer thickness at pole	15 mm
Shell thickness	6.35 mm
Beam tube o.d., bare	(4.763 in.) 121 mm
Beam tube wall thickness	(0.157 in.) 4 mm
Beam tube/coil radial gap	(0.175 in.) 4.4 mm
Operating Temperature	4.6 K
Design current	5.05 kA
Design gradient	48.1 T/m
Computed quench current	8.26 kA
Computed quench gradient	75.3 T/m
Field margin	57 %
Inductance	13 mH
Stored energy in Q2 @ design current	165 kJ
Transfer function	
at low current	9.57 T/m/kA
at design gradient	9.52 T/m/kA

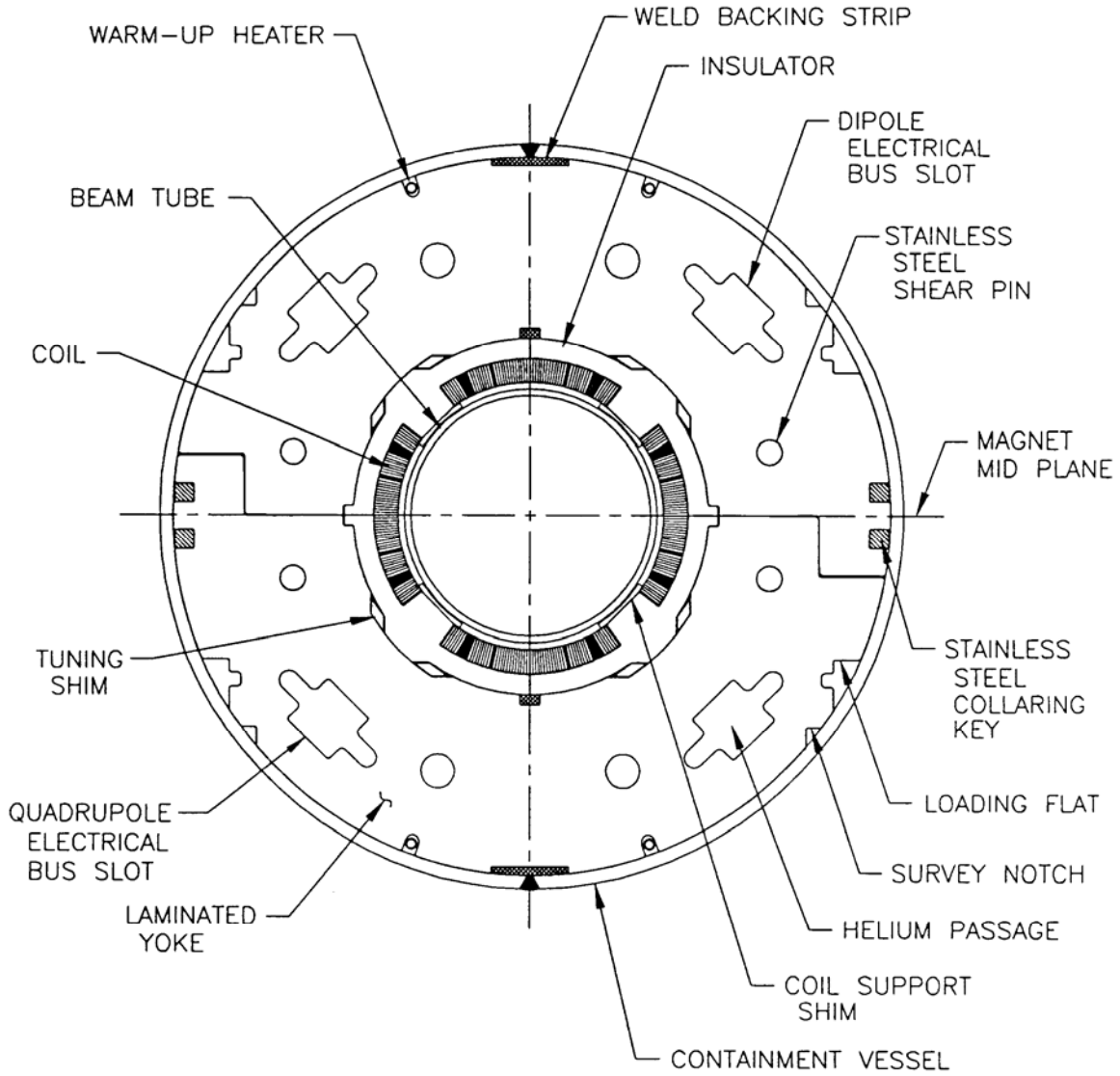


Fig. 10-1. Cross section of 13 cm quadrupole (coil i.d. = 130 mm).

The 13 cm Coil Cross-section

The coil consists of three blocks with 13, 8 and 6 turns, for a total of 27 turns/pole, all with Kapton CI insulation. The larger wedge is a section of an annulus, and the smaller wedge is rectangular. That is, the wedges are chosen to be mechanically symmetric instead of being an exact (but asymmetric) match to the variable radius geometry. The coil cross-section is shown in Fig. 10-2 .

The coil design QRI D86F is based on an insulated cable mid-thickness of 1.346 mm (0.0530 in.) and width of 12.01 mm and is an iteration of a previous design. It is optimized to give quadrupole harmonics (at 40 mm radius) of $b_{5'} = -31.4$ and $b_{9'} = 0.8$ with a circular, infinite- μ iron aperture. These non-zero harmonics are partly intended to compensate for the non-circular iron aperture, partly to compensate for the differences between calculations and measurements in QRI001 and QRI002 at the design maximum current and, in the case of b_5 , partly to compensate for the effects of the leads.

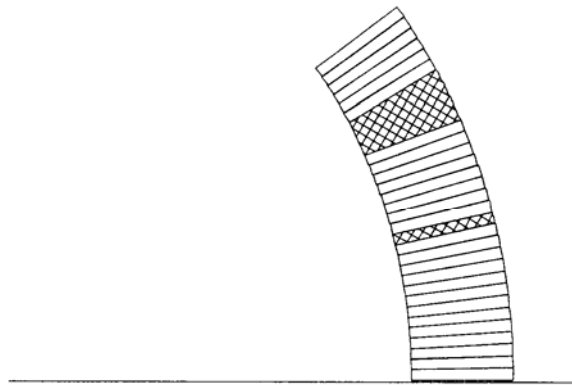


Fig. 10-2 . Iterated coil cross-section and parameters for the RHIC 13 cm aperture insertion quadrupole.

Iron Cross-section

The yoke outer diameter is 350.5 mm. The inner radius of the yoke is 87 mm from midplane to $\theta = 25.8^\circ$, at which angle there is a vertical taper to a radius of 92 mm, with symmetry around a 45° radial line. The angle and the difference between the radii are used as parameters in minimizing $b_{3'}$ saturation. The locating notch at the midplane is 5 mm deep and 10 mm wide. Some other structures in the yoke are shown in Fig. 10-1; although these other structures break a strict quadrupole symmetry, the location of them is such that their influence is minimal. The first sign of symmetry breaking due to this iron geometry is the appearance of b_9 at high current. Nonmagnetic tie rods and shear pins have been located in such a way that $b_{3'}$ is <0.1 at the design current.

The change in the allowed harmonics $b_{3'}$ and $b_{6'}$ due to single magnet iron saturation is about 0.3 unit at design current (5 kA) and about 1 unit at quench current (~ 8.6 kA). The higher order allowed harmonics remain practically constant up to quench excitation.

At the ends nearest the crossing point, Q1 in the inner arc and Q1 in the outer arc are separated by ~ 61 mm. This is close enough to break the quadrupole symmetry at the higher excitations, resulting in additional field dependent harmonics.

In RHIC, the ratio of beam rigidities can vary from 1:1 to $\sim 2.5:1$. In the anti-symmetric RHIC lattice, the cross talk is maximum when both quadrupoles are excited at high current (1:1 case). The separation increases along the length of the quadrupoles; thus the effect is maximum at the crossing point ends. The dominant cross talk induced harmonic $b_{6'}$ is about 0.1 unit at design currents, and is less than 1 unit at quench currents, according to calculations using POISSON and PE2D. The value of $b_{6'}$ varies significantly over the length of Q1. The computed change in $b_{3'}$ due to non-symmetric iron yoke and cross talk is about 0.1 unit at the design current and about 0.3 unit at quench. All other saturation cross talk harmonics are less than 0.05 unit at design currents, and are less than 1 unit at quench currents.

Post-Construction Harmonic Correction

The desired harmonics in these magnets are much smaller than can be obtained with normal construction techniques. To reduce the measured values of harmonics b_i and a_i , $i = 2, 3, 4$ and 5 , eight tuning shims were placed at the inner surface of the iron of each quadrupole after magnetic measurements have been made at room temperature. The actual tuning shim is a package of a number of low carbon steel (magnetic) and brass (non-magnetic) laminations with a total thickness

of 6.35 mm. The nominal magnetic thickness of a tuning shim is 3.175 mm, but the actual value could be anywhere between the range of 0.0 and 6.35 mm to reduce the measured harmonics. These tuning shims were inserted in the eight spaces symmetrically located between the plastic spacer and the iron yoke. In the first octant, this parallelogram-shaped space is at about 30° and is between the radii of 87 and 92 mm.

Coil and Lead Modifications Added After Testing

Measurements on the first two magnets built, QRI001 and QRI002, revealed that quadrupole symmetry was not realized during construction. To compensate for this, the coil-to-coil gaps at 0° and 180° were increased to 0.25 mm and those at 90° and 270° to 0.15 mm.

Measurements also showed substantial harmonics, both normal and skew, in the lead end due to placement of the 8 leads after they exit the coil proper. It was found that this could be ameliorated by rotating all 8 leads (which alternate in current direction) 90° azimuthally in the magnet end space in such a way that roughly equal lengths of lead, with opposing current direction, occupy each azimuthal position. The integrated harmonics in this space were thereby reduced or eliminated.

The tuning shim packages were adjusted to reduce the measured values of the normal and skew sextupole, octupole, decapole, and dodecapole harmonics, based on the room temperature measurements.

Results for the quench tests of the insertion quadrupoles are shown in Fig. 10-3. The first quenches of all but two of the magnets were above the 5 kA operating current. Later test protocol limited ramping to 7 kA. Quench origins were studied with both voltage taps and a quench antenna [OG96], but no single location was identified as limiting the performance. Additional quench testing was performed to verify that the magnets did not retrain after a thermal cycle. All of the Q1's and Q2's were cold tested, but only 13 of the Q3's. None of the insertion quads has quenched in RHIC.

Plots of the transfer function and first allowed harmonic versus current are given for a Q1 (Figs. 10-4 and 10-5), a Q2 (Figs. 10-6 and 10-7), and a Q3 (Figs. 10-8 and 10-9). The magnets shown are those closest to the mean for that length.

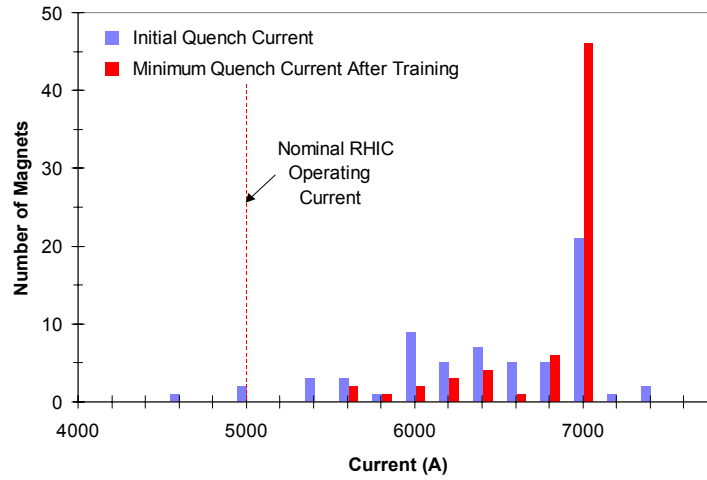


Fig. 10-3. Quench performance of 61 large aperture (130 mm) quadrupoles, tested at 4.5 K.

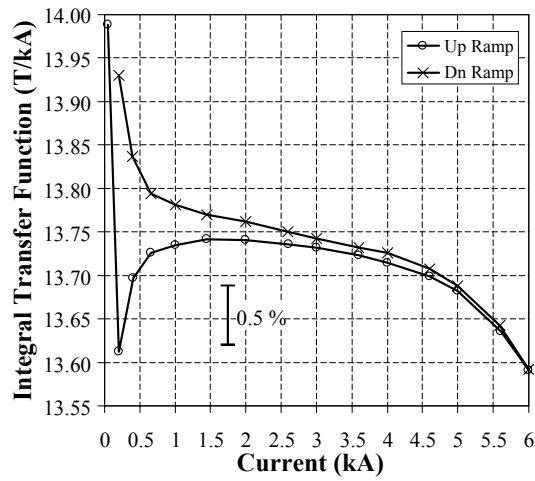


Fig. 10-4. Integral transfer function in Q1 magnet QRI14 (close to mean at 5 kA).

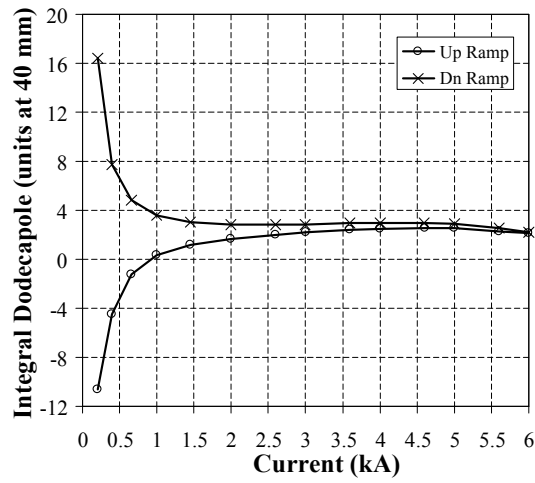


Fig. 10-5. Integral first allowed harmonic (b_5) in Q1 magnet QRI114.

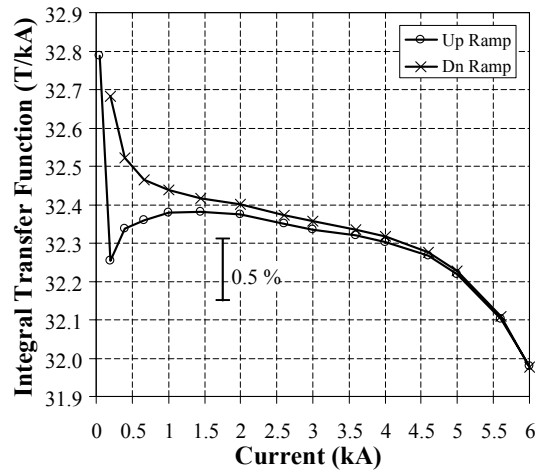


Fig. 10-6. Integral transfer function in Q2 magnet QRK119 (close to mean at 5 kA).

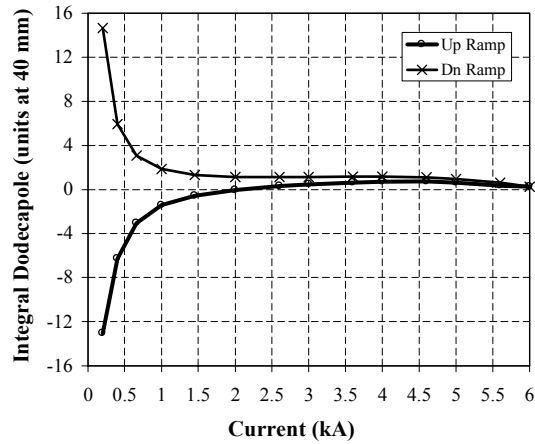


Fig. 10-7. Integral first allowed harmonic (b_5) in Q2 magnet QRK119.

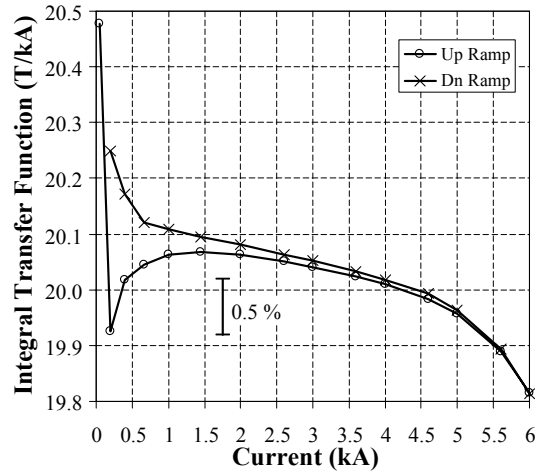


Fig. 10-8. Integral transfer function in Q3 magnet QRJ116 (close to mean at 5 kA).

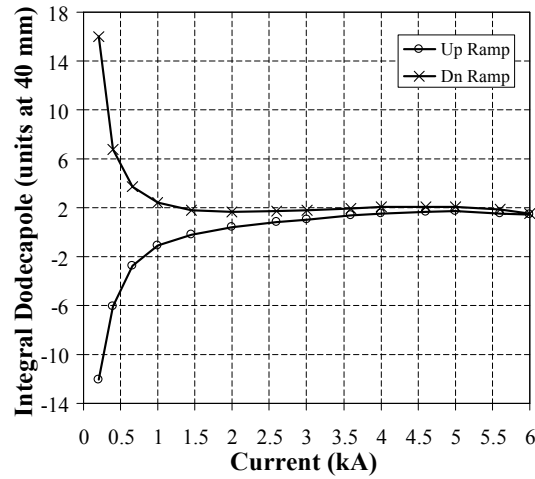


Fig. 10-9. Integral first allowed harmonic (b_5) in Q3 magnet QRJ116.

Tuning shims were used to optimize the field quality at 5 kA, where the quadrupoles play the greatest role in beam performance. The use of tuning shims significantly improved the field quality of the quadrupoles, particularly for the low order terms (Fig. 10-10) [GU99]. There were several practical limitations to improving the field quality with the tuning shims. One is the uncertainty in the correlation between warm and 5 kA measurements. Saturation reduces the correlation with measurements made at lower currents. Figures 10-11 and 10-12 show this effect for the normal sextupole. Also, warm-cold correlations must be established for each length of quadrupole, significantly lengthening the cold test time needed for the first magnets of each type. Another limitation is the change in harmonics with quenching or thermal cycle. Magnetic measurements were made before and after quench and thermal cycles on eight of the Q1's that were thermally cycled [GU97]. The rms of the change in the low-order harmonics due to quenching and thermal cycling was several tenths of a unit, somewhat smaller than the uncertainty in the warm-cold correlation.

The difference in the field quality requirements for the two “golden” IR's ($\beta^* = 1\text{m}$) and the other four “non-golden” regions ($\beta^* = 10\text{m}$) made it possible to use all of the quadrupoles built in RHIC [WE99]. Nearly all of the quadrupoles met the field requirements for “golden” IR's. The integral field quality data at 5 kA for all the magnets tested cold are given in Table 10-2. In early magnets of the Q1 and Q3 series, the first allowed harmonic, b_5 , was larger than in later magnets.

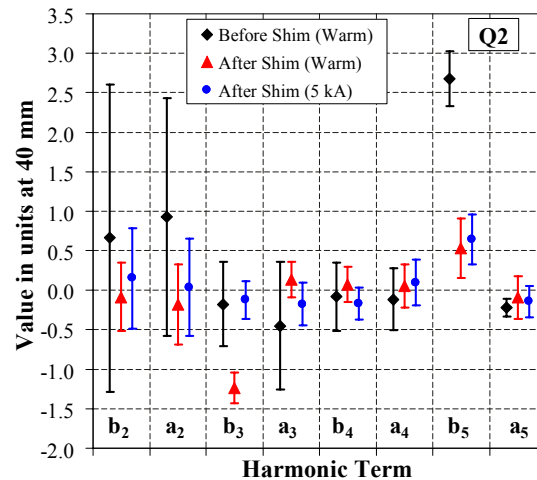


Fig. 10-10. Harmonics before and after shimming in the Q2 quads (QRK).

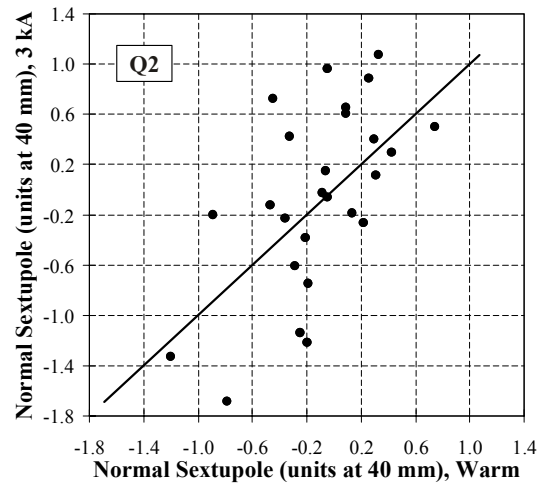


Fig. 10-11. Warm-cold correlation of b2 in the Q2 (QRK) magnets at 3 kA.

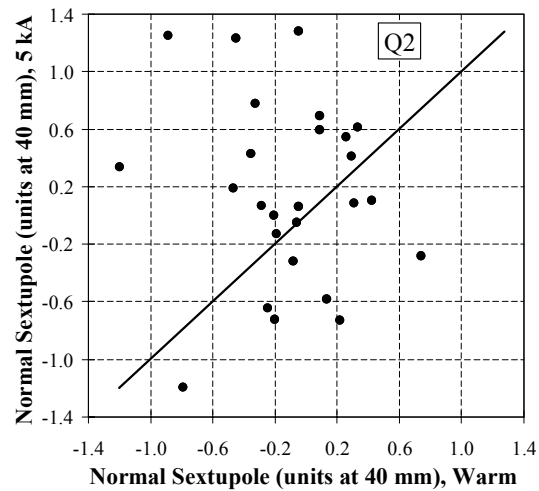


Fig. 10-12. Warm-cold correlation of b2 in the Q2 (QRK) magnets at 5 kA (shim saturation).

Table 10-2. Summary of integral field quality data in 130 mm aperture insertion quadrupoles.

Harmonic at 40 mm	Mean at 5 kA			Standard Deviation at 5 kA		
	Q1 (1.44 m) (26 magnets)	Q2 (3.4 m) (27 magnets)	Q3 (2.1 m) (13 magnets)	Q1 (1.44 m) (26 magnets)	Q2 (3.4 m) (27 magnets)	Q3 (2.1 m) (13 magnets)
ITF(T/kA)	13.658	32.170	19.954	0.32%	0.13%	0.06%
b ₂	0.14	-0.08	0.01	0.44	0.43	0.73
b ₃	-0.14	-1.24	-0.34	0.44	0.19	0.51
b ₄	0.02	0.08	-0.23	0.25	0.22	0.23
b ₅	2.15	0.53	1.67	0.59	0.38	0.13
b ₆	0.03	0.02	0.07	0.22	0.19	0.17
b ₇	-0.14	-0.14	0.00	0.18	0.09	0.13
b ₈	0.02	0.00	0.05	0.05	0.05	0.06
b ₉	-0.10	-0.37	-0.31	0.17	0.07	0.03
b ₁₀	0.00	0.00	0.00	0.02	0.02	0.01
a ₂	-0.23	-0.18	0.40	0.56	0.51	0.59
a ₃	-0.02	0.13	0.12	0.25	0.22	0.33
a ₄	-0.08	0.05	0.06	0.29	0.28	0.15
a ₅	-0.74	-0.09	-0.27	0.12	0.27	0.07
a ₆	0.20	0.13	0.09	0.29	0.22	0.19
a ₇	-0.04	-0.01	-0.01	0.08	0.10	0.07
a ₈	-0.02	0.00	0.01	0.05	0.06	0.03
a ₉	0.18	0.05	0.08	0.02	0.02	0.02
a ₁₀	0.01	0.00	0.01	0.02	0.02	0.02